

Selective Inhibition of Endoplasmic Reticulum-associated Degradation Rescues Δ F508-Cystic Fibrosis Transmembrane Regulator and Suppresses Interleukin-8 Levels

THERAPEUTIC IMPLICATIONS*

Received for publication, January 18, 2006, and in revised form, March 30, 2006 Published, JBC Papers in Press, April 18, 2006, DOI 10.1074/jbc.M600509200

Neeraj Vij[‡], Shengyun Fang[§], and Pamela L. Zeitlin^{‡,1}

From the [‡]Division of Pediatric Respiratory Sciences, Johns Hopkins School of Medicine, Baltimore, Maryland 21287 and the [§]Medical Biotechnology Center, University of Maryland Biotechnology Institute, Baltimore, Maryland 21201

Endoplasmic reticulum (ER)-associated degradation (ERAD) is the major quality control pathway of the cell. The most common disease-causing protein folding mutation, Δ F508-cystic fibrosis transmembrane regulator (CFTR), is destroyed by ERAD to cause cystic fibrosis (CF). p97/valosin-containing protein (VCP) physically interacts with gp78/autocrine motility factor receptor to couple ubiquitination, retrotranslocation, and proteasome degradation of misfolded proteins. We show here that p97/VCP and gp78 form complexes with CFTR during translocation from the ER for degradation by the cytosolic proteasome. Interference in the VCP-CFTR complex promoted accumulation of immature CFTR in the ER and partial rescue of functional chloride channels to the cell surface. Moreover, under these conditions, interleukin-8 (IL8), the expression of which is regulated by the proteasome, was reduced. Inhibition of the proteasome with bortezomib (PS-341/Velcade) also rescued CFTR, but with less efficiency, and suppressed NF κ B-mediated IL8 activation. The inhibition of the major stress-inducible transcription factor CHOP (CCAAT/enhancer-binding protein homologous protein)/GADD153 together with bortezomib was most effective in repressing NF κ B-mediated IL8 activation compared with interference of VCP, MLN-273 (proteasome inhibitor), or 4-phenylbutyrate (histone deacetylase inhibitor). Immunoprecipitation of Δ F508-CFTR from primary CF bronchial epithelial cells confirmed the interaction with VCP and associated chaperones in CF. We conclude that VCP is an integral component of ERAD and cellular stress pathways induced by the unfolded protein response and may be central to the efficacy of CF drugs that target the ubiquitin-proteasome pathway.

Endoplasmic reticulum (ER)²-associated protein degradation (ERAD) eliminates misfolded, damaged, or mutant proteins with abnormal conformation (1). ERAD targets are selected by a quality control system within

the ER lumen and are ultimately destroyed by the cytoplasmic ubiquitin-proteasome system. The ubiquitin-proteasome system plays a pivotal role in cell homeostasis and is vital in regulating various cellular processes. In normal cells, nearly all proteins are continuously degraded and replaced by *de novo* synthesis. The spatial separation between substrate selection and degradation in ERAD requires substrate transport from the ER to the cytoplasm by a process termed dislocation, recently reviewed by Meusser *et al.* (2).

The most common disease-causing protein folding mutation is deletion of phenylalanine at position 508 of the cystic fibrosis transmembrane regulator (Δ F508-CFTR), which results in a temperature-sensitive folding defect and premature degradation by ERAD (3). The absence of CFTR at the airway epithelial cell surface disrupts luminal hydration and is associated with an exaggerated immune response (4). Functional CFTR can be restored by growth at lower temperature (25–27 °C) or incubation with chemical chaperones, which rescues Δ F508-CFTR from ERAD (5).

Mammalian p97/valosin-containing protein (VCP) and its yeast counterpart, Cdc48, participate in retrotranslocation of misfolded proteins from the ER for degradation by the cytosolic proteasomes (6). p97/VCP and its cofactors (Ufd1, Npl4, and p47) interact with misfolded ubiquitinated substrates to dislodge them from the ER to the cytosol for proteasome degradation (7). We have reported recently that p97/VCP physically interacts with gp78 to couple ubiquitination, retrotranslocation, and proteasome degradation (8). Originally identified as the tumor autocrine motility factor receptor, gp78 is a multimembrane-spanning protein with RING finger-type ubiquitin-protein ligase activity exposed to the cytoplasmic ER surface. gp78/autocrine motility factor receptor is thus distinguished from CHIP (C terminus of Hsc70-interacting protein) and Parkin ubiquitin-protein ligases and closely resembles the yeast ERAD ubiquitin-protein isopeptide ligase Hrd1p/Der3p. In yeast, Hrd1p/Der3p and Cdc48 are required for CFTR degradation (9). We hypothesize that selective inhibition of ERAD not only rescues Δ F508-CFTR, but also suppresses interleukin (IL)-8 levels, the major inflammatory cytokine in cystic fibrosis (CF) airways.

EXPERIMENTAL PROCEDURES

Human Subjects—CF (homozygous for Δ F508-CFTR; $n = 3$, 7–9 years old) and non-CF ($n = 3$, 8–17 years old) subjects who were undergoing fiberoptic bronchoscopy and bronchoalveolar lavage (BAL) for a clinical indication were invited to participate in a Johns Hopkins Institutional Review Board- and General Clinical Research Center-approved protocol. All three children with CF were chronically infected with one or more bacteria. The non-CF subjects were children with airway pathology: 1) a case of focal bronchiectasis from an earlier *Mycoplasma*

* This work was supported by National Institutes of Health Grant RO1 HL59410. IB3-1 cells are under a licensing agreement between Pfizer Inc., Japan Tobacco Inc., and The Johns Hopkins University. Dr. Zeitlin is entitled to a fee received by the University on sales of this cell line. The terms of this arrangement are being managed by the University in accordance with its conflict of interest policies. The costs of publication of this article were defrayed in part by the payment of page charges. This article must therefore be hereby marked "advertisement" in accordance with 18 U.S.C. Section 1734 solely to indicate this fact.

¹ To whom correspondence should be addressed: Dept. of Pediatrics, Johns Hopkins School of Medicine, 600 N. Wolfe St., Park 316, Baltimore, MD 21287. Tel.: 410-614-5637; Fax: 410-955-1030; E-mail: pzeitlin@jhmi.edu.

² The abbreviations used are: ER, endoplasmic reticulum; ERAD, endoplasmic reticulum-associated protein degradation; CFTR, cystic fibrosis transmembrane regulator; VCP, valosin-containing protein; IL, interleukin; CF, cystic fibrosis; BAL, bronchoalveolar lavage; 4-PBA, 4-phenylbutyrate; wt, wild-type; GFP, green fluorescent protein; shRNA, short hairpin RNA; CFTE, cystic fibrosis tracheal epithelial; MQAE, *N*-(ethoxycarbonylmethyl)-6-methoxyquinolinium bromide; UPR, unfolded protein response; UPS, ubiquitin-proteasome system.

Selective Inhibition of ERAD Rescues Δ F508-CFTR

pneumoniae infection (the BAL fluid was culture-positive for *Branhamella catarrhalis*, and the cytopathology contained neutrophils and lipid-laden macrophages); 2) a case of chronic lung disease and yellow nail syndrome (culture-positive for *Hemophilus influenzae* and associated with neutrophils and lipid-laden macrophages upon BAL); and 3) a case of psychogenic cough (culture-negative and associated with lipid-laden macrophages upon BAL). Except for the case of psychogenic cough, there was a mild inflammatory phenotype. Parents signed informed consent on behalf of their children. Bronchial brushings were obtained after BAL to minimize contamination with mucus and neutrophils. Brushes were directly immersed in cell culture medium on ice for later transport to the laboratory.

Investigational Therapeutics—The proteasome inhibitors bortezomib or PS-341 or Velcade (Johns Hopkins Pharmacy) and MLN-273 (under a material transfer agreement) were from Millenium Pharmaceuticals, Inc. (Cambridge, MA), and 4-phenylbutyrate (4-PBA) was from Sigma.

Antibodies and Plasmids—Rabbit anti-CFTR 169 and anti-gp78 polyclonal antibodies have been described previously (8, 10). Mouse/rabbit anti-VCP polyclonal antibodies from Affinity BioReagents (Golden, CO) and Santa Cruz Biotechnology, Inc. (Santa Cruz, CA) were used. Anti-Hsp90 (rat monoclonal), anti-Hsp70 (mouse monoclonal/rabbit polyclonal), anti-Hsc70 (rabbit polyclonal), and anti-Hsp40 (rabbit polyclonal) antibodies were purchased from Stressgen Biotechnologies Corp. (San Diego, CA). Rabbit anti-CHIP polyclonal antibody was obtained from Abcam Inc. (Cambridge, MA). The plasmid constructs pCIneo-gp78, pCIneo-gp78C, and VCPQQ have been described previously (8). Δ F508-CFTR-green fluorescent protein (GFP) and wild-type (wt) CFTR-GFP were constructed in the pS65T-C1 vector. VCP short hairpin RNA (shRNA) was constructed in the pSM2 vector (Open Biosystems, Huntsville, AL). Briefly, the single oligonucleotide containing the hairpin and common 5'- and 3'-ends was used as a PCR template. The oligonucleotide was PCR-amplified using universal primers containing XhoI (5') and EcoRI (3') sites. The PCR fragment was then cloned into the hairpin cloning site of pSM2. The VCP anti-sense/target sequence 22-mer is shown in boldface, and common microRNA-30 context regions are shown in italics below. The VCP shRNA was amplified using the Advantage-GC PCR kit (Qiagen Inc.) with a single-strand 97-nucleotide "microRNA-30-like" DNA template oligonucleotide (*TGCTGTTGACAGTGAGCGCCCGCAAGAAGATGGATCTCATTAGTGAAGCCACAGATGTAATGAGATCCATCTTCTTGCGGATGCCTACTGCCTCGGA*) and primers 5'-miR30PCR_{XhoI} (CAGAAAGGCTCGAGAAGGTATATGCTGTTGACAGTGAGCG) and 3'-miR30PCRE_{EcoRI} (CTAAAGTAGCCCTTGAATTCCGAGGCAGTAGGCA). PCR conditions were as follows: 94 °C for 30 s, 94 °C for 30 s, and 55 °C for 30 s for 25 cycles; 75 °C for 10 min; and 4 °C forever). The CHOP (CCAAT/enhancer-binding protein homologous protein) shRNA was purchased from Open Biosystems.

Cell Culture, Transfection, and Metabolic Labeling—IB3-1 cells (Δ F508/W1282X, low level expression of Δ F508-CFTR and no W1282X-CFTR protein), CF tracheal epithelial (CFTE) cells (homozygous for Δ F508-CFTR), and S9 cells (IB3-1 cells corrected with adeno-associated virus-CFTR) were maintained in LHC-8 medium (BIOSOURCE) containing 100 units/ml penicillin, 100 μ g/ml streptomycin, 0.25 μ g/ml amphotericin B, and 10% fetal bovine serum (all from Invitrogen). The cells were plated on 6-well plates, transfected with 4 μ g of each Δ F508/wt-CFTR-GFP plasmid DNA, and cotransfected with the VCP shRNA (Δ VCP), VCPQQ (deficient in AAA ATPase domains D1 and D2), gp78 small interfering RNA (Δ gp78), or gp78 Δ C (deficient in the VCP-binding domain) construct using Lipofectamine 2000 (Invitrogen) as recommended by the manufacturer. After 48 h of trans-

fection, cells were rinsed three times and starved for 1 h in methionine- and cysteine-free Dulbecco's modified Eagle's medium. Cells were pulse-labeled with 250 μ Ci/ml [³⁵S]methionine/cysteine (ICN Biomedical, Irvine, CA) for 30 min and then chased in Dulbecco's modified Eagle's medium containing 10 mM methionine and 4 mM cysteine for the indicated times.

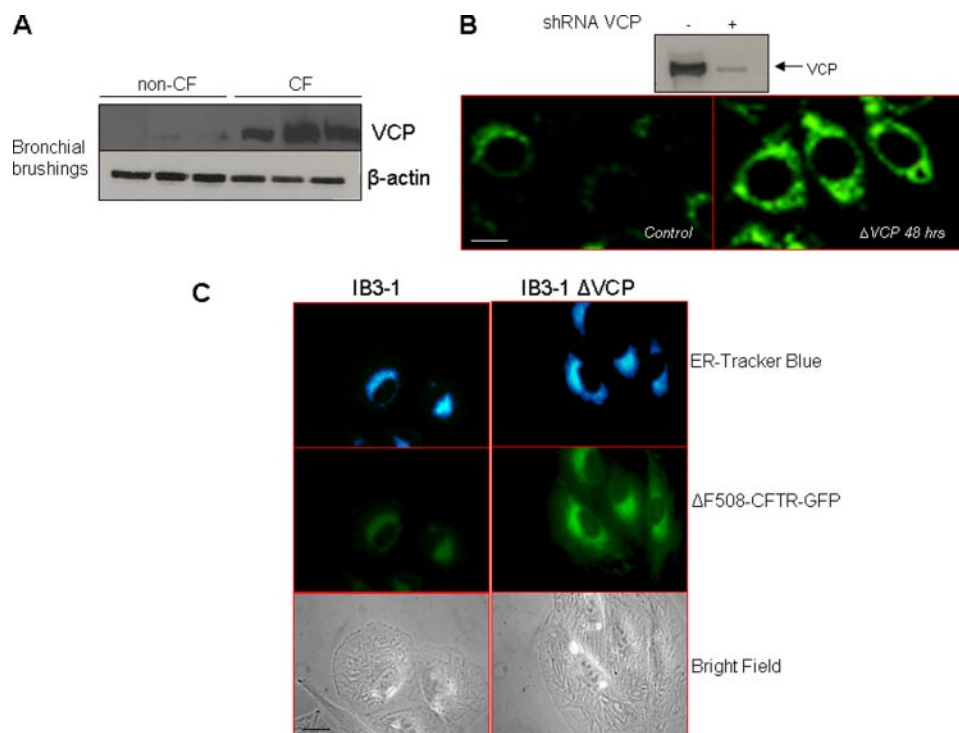
Fluorescence Microscopy—After 48 h of transfection, cells were washed three times with Hanks' balanced salt solution containing calcium and magnesium (Invitrogen) and loaded with 1 μ M ER-TrackerTM Blue-White DPX dye (Invitrogen). Plates were incubated at 37 °C and 5% CO₂ for 2 h and examined under a Zeiss Axiovert 135-N fluorescence microscope. A Quantix 1401 charge-coupled device camera and IPLab software Version 3.5 with appropriate filter settings for GFP (fluorescein isothiocyanate) or ER-Tracker Blue (4',6-diamidino-2-phenylindole) were used to capture the images.

Immunoprecipitation and Immunoblotting—Cells were lysed directly on plates using M-PER protein lysis buffer (Pierce) containing protease inhibitor mixture (Roche Applied Science) after three washes with ice-cold phosphate-buffered saline. CF bronchial brushings were transferred to lysis buffer. For immunoprecipitation, total protein extracts (500 μ g/ml for cell culture and 50 μ g/ml for bronchial brushings) were incubated with 50 μ l of protein A/G-agarose beads (Santa Cruz Biotechnology, Inc.) for 3 h at 4 °C. After preclearing, 5 μ g of respective primary antibody or preimmune serum (negative control) was added to each tube. After 1 h, protein A/G-agarose beads (50 μ l) were added to each tube, and tubes were incubated overnight at 4 °C. Beads were washed once with lysis buffer (20 mM Tris-HCl (pH 7.6), 150 mM NaCl, 0.5% Triton X-100, and 10 μ M phenylmethylsulfonyl fluoride), followed with two washes with phosphate-buffered saline. The beads were suspended in Laemmli sample buffer (30 μ l) containing β -mercaptoethanol, vortexed for 1 min, resolved by 4–10% SDS-PAGE, and transferred to a 0.4- μ m pore size nitrocellulose membrane. Proteins were detected using the respective primary antibodies. For pulse-chase experiments, CFTR immunoprecipitate was eluted with sample buffer and separated on a 4–8% SDS-polyacrylamide gel, dried for 2 h, and processed for autoradiography.

IL8 Cytokine Enzyme-linked Immunosorbent Assay—IB3-1 cells were transfected with the Δ VCP, VCPQQ, Δ gp78, or gp78 Δ C construct and treated with 5 μ M bortezomib or 5 mM 4-PBA. At 24 h post-transfection, the cells were induced with 1 ng/ml IL1 β . After 48 h of transfection, supernatants were collected, and IL8 levels were measured by solid-phase enzyme amplified sensitivity immunoassay (BIOSOURCE) as specified by the manufacturer. Standards and high and low cytokine controls were included. The plates were read at 450 nm on a 96-well microplate reader (Molecular Devices Corp.) using SoftMax Pro software. The mean blank reading was subtracted from each sample and control reading. The amount of substrate turnover was determined calorimetrically by measuring the absorbance proportional to IL8 concentration. A standard curve was plotted, and an IL8 concentration in each sample was determined by interpolation from the standard curve. The data represent the means \pm S.D. of three independent experiments.

NoShift NF κ B Binding Assay—IB3-1 cells transfected (24 h) with Δ VCP, Δ F508-CFTR, or Δ CHOP were treated with 5 μ M bortezomib (6 h), 5 μ M MLN-273 (6 h), or 5 mM 4-PBA (24 h). Cells were induced with IL1 β (1 ng/ml) for 12 h. After 24 h of transfection, nuclear extracts (11) were collected using a NucBuster protein extraction kit (Novagen, San Diego, CA), and the shift in bound NF κ B was measured using a NoShift NF κ B binding assay kit (Novagen) as specified by the manufacturer. The signal from nuclear extracts was compared with the negative control (minus the extract). The specificity of protein binding was established using NF κ B-specific and mutant competitors. The plates were read at

FIGURE 1. Inhibition of p97/VCP expression results in accumulation of CFTR in the ER. *A*, total protein extract (10 μ g) from freshly isolated bronchial epithelial cells obtained upon bronchoscopy from $\Delta F508$ CF subjects and non-CF controls was immunoblotted for VCP and β -actin. VCP is overexpressed in CF airways. *B*, IB3-1 cells were transfected with $\Delta F508$ -CFTR-GFP and cotransfected with VCP shRNA (Δ VCP). The Δ VCP efficiency is shown in the upper panel, in which the VCP protein level was drastically decreased by Δ VCP (+) compared with the control lane (–) (20 μ g in each lane). In a parallel experiment in the lower panels, $\Delta F508$ -CFTR-GFP accumulated in a perinuclear location when VCP was decreased. *C*, IB3-1 cells transfected with $\Delta F508$ -CFTR-GFP and/or Δ VCP were loaded with ER-Tracker Blue-White DPX. The localization of ER-Tracker Blue dye and $\Delta F508$ -CFTR-GFP is shown in upper and middle panels, respectively. The lower panel shows the bright-field image of the area indicating the normal morphology of cells after VCP inhibition. Co-localization of ER-Tracker Blue dye and $\Delta F508$ -CFTR-GFP demonstrated accumulation of $\Delta F508$ -CFTR in the ER. VCP inhibition augmented $\Delta F508$ -CFTR accumulation in the ER, and part of it appeared to escape from the ER in Δ VCP IB3-1 cells. Scale bar = 20 μ m.



450 nm on a 96-well microplate reader using SoftMax Pro software. The absorbance readings were used to determine the levels of bound NF κ B. The data represent the means \pm S.D. of three independent experiments.

N-(Ethoxycarbonylmethyl)-6-methoxyquinolinium Bromide (MQAE) Assay—CFTR-mediated chloride transport activity in IB3-1 cells transfected with the Δ VCP, VCPQQ, Δ gp78, or gp78 Δ C construct and treated with bortezomib (1, 5, or 10 μ M) was assayed using the halide-sensitive dye MQAE. Fluorescence of MQAE is quenched by halides. Cells were grown on glass coverslips in Dulbecco's modified Eagle's medium containing 10% fetal bovine serum. Cells were loaded with the dye by hypotonic shock at 37 $^{\circ}$ C for 40 min in Opti-MEM/water (1:1) containing 10 mM MQAE, washed, and then mounted in a perfusion chamber for fluorescence measurements. Fluorescence was measured using a Zeiss inverted microscope coupled to a charge-coupled device camera. Excitation and emission wavelengths were 350 and 460 nm, respectively. The stage and objective lenses were maintained at 37 $^{\circ}$ C. The medium was kept flowing through the perfusion chamber at 1 ml/min using a peristaltic pump. Both 10 μ M forskolin and 10 μ M genistein were used to induce Cl $^{-}$ transport in IB3-1 cells. CFTR was inhibited with either 5 μ M CFTR inhibitor-172 (12) or myristoylated protein kinase A inhibitor 14–22 amide (Calbiochem) to reduce cAMP-mediated phosphorylation. Chloride efflux was calculated using Equations 1–3.

$$F_0/F_{Cl} = 1 + [Cl^{-}]_i \cdot K_{SV} \quad (\text{Eq. 1})$$

$$F_0 = F_{20} \cdot (1 + 0.02 \cdot K_{SV}) \quad (\text{Eq. 2})$$

$$dCl/dt = F_0/(K_{SV} \cdot (F_{Cl})^2) \cdot dF_{Cl}/dt \quad (\text{Eq. 3})$$

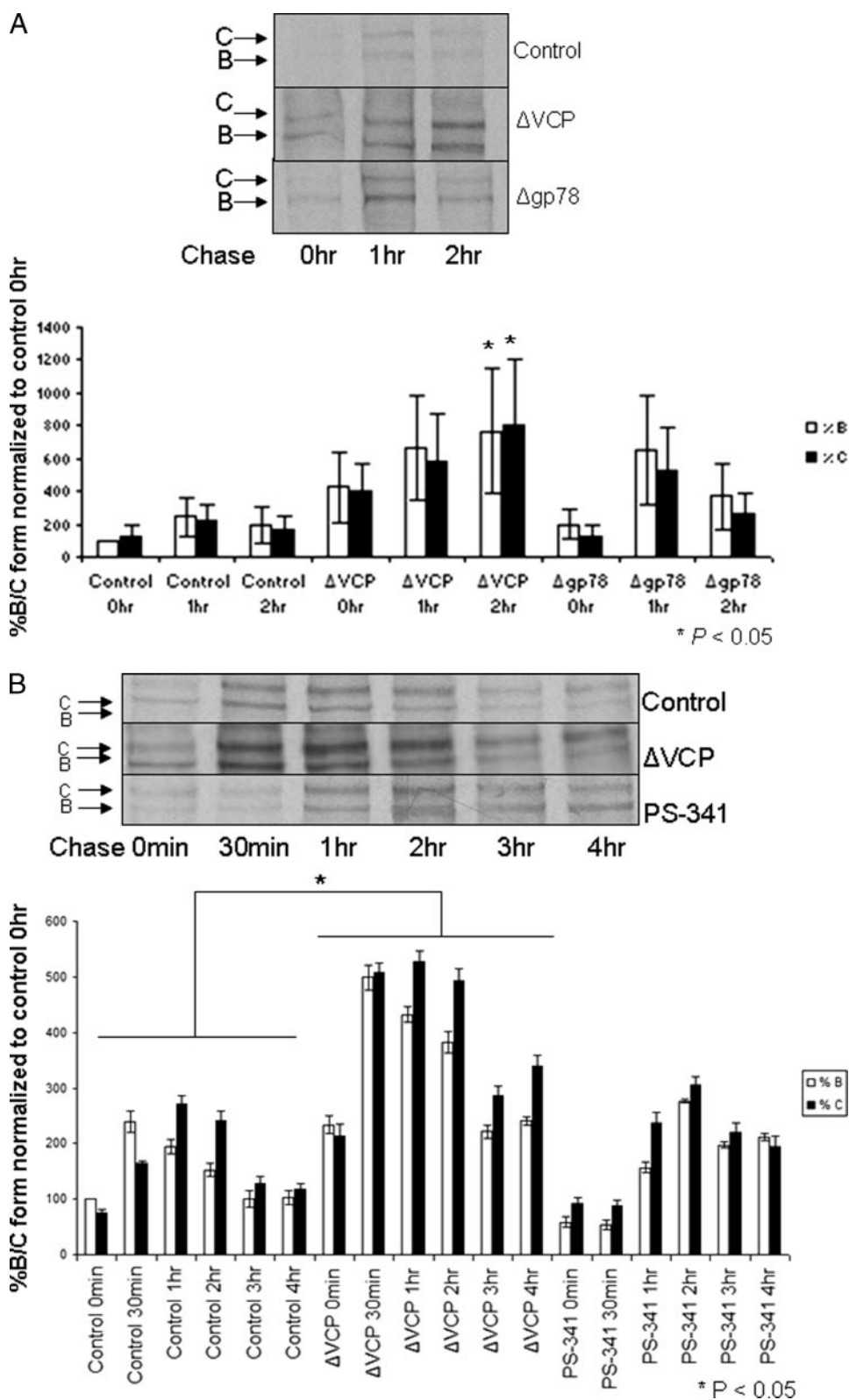
Statistical Analysis—All data are represented as the means \pm S.D. of three experiments. One-way analysis of variance with Dunnett's planned comparison was run for each sample versus the control. A *p* value <0.05 was considered to have statistical significance.

RESULTS

p97/VCP Participates in ERAD of $\Delta F508$ -CFTR—To test the hypothesis that VCP is involved in $\Delta F508$ -CFTR degradation, we first estimated VCP protein levels in freshly isolated bronchial epithelial cells from $\Delta F508$ CF and non-CF subjects. As expected, VCP levels were up-regulated in all $\Delta F508$ CF subjects compared with non-CF controls (Fig. 1A). Moreover, the difference between CF and non-CF bronchial expression was striking. We next hypothesized that transient knock-down of either VCP or gp78 would rescue $\Delta F508$ -CFTR from ERAD in CF bronchial epithelial cells. To reduce the expression of these proteins, we constructed short hairpin/small interfering RNA. The efficiency of VCP shRNA (Δ VCP)-mediated inhibition of VCP protein levels in IB3-1 cells ($\Delta F508$ /W1282X CF bronchial epithelial line) (13) was evaluated by immunoblotting of whole cell lysates (Fig. 1B, upper panel). To localize $\Delta F508$ -CFTR signal, the IB3-1 cells were transfected with $\Delta F508$ -CFTR-GFP and cotransfected with Δ VCP or a plasmid control. Inhibition of VCP was associated with accumulation of $\Delta F508$ -CFTR-GFP in the ER compared with the control (Fig. 1B, lower panels). Accumulation of $\Delta F508$ -CFTR in the ER was confirmed by co-localization of the GFP signal with the signal from ER-Tracker Blue-White DPX. Furthermore, spreading of the GFP signal beyond the ER tracker dye compartment suggested that $\Delta F508$ -CFTR-GFP escaped from the ER in Δ VCP IB3-1 cells (Fig. 1C).

p97/VCP Inhibition Rescues $\Delta F508$ -CFTR from ERAD—In IB3-1 cells, the ER-retained $\Delta F508$ -CFTR protein is core-glycosylated (160-kDa immature B form), whereas growth at 26 $^{\circ}$ C allows the $\Delta F508$ -CFTR protein to transit the biosynthetic pathway and to acquire complex glycosylation (180-kDa mature C form) (5). Moreover, the $\Delta F508$ -CFTR band C form has a faster turnover rate from the plasma membrane (14). To assess the effects of Δ VCP on the stability of $\Delta F508$ -CFTR bands B and C, IB3-1 cells were first transiently transfected with $\Delta F508$ -CFTR-GFP for 48 h and then metabolically labeled with [35 S]methionine. $\Delta F508$ -CFTR was immunoprecipitated with anti-CFTR antibody 169 (15) after the indicated chase time (Fig.

Selective Inhibition of ERAD Rescues $\Delta F508$ -CFTR



2A, Control). Cotransfection with ΔVCP (Fig. 2A) resulted in stabilization of both B and C forms. By comparison, cotransfection with gp78 small interfering RNA ($\Delta\text{gp}78$) produced only a transient rescue of the mature C form with a peak at 1 h (Fig. 2A), suggesting that VCP (not gp78) is central to extraction of CFTR from the ER for ERAD. S9 cells (IB3-1 cells corrected with wt-CFTR) were similarly transfected with

additional wt-CFTR and ΔVCP . We observed an efficient maturation and stability of band B to band C (Fig. 2B), confirming that wt-CFTR and $\Delta F508$ -CFTR are extracted and degraded through the same VCP-mediated pathway.

We considered the proteasomal compartment as a potential therapeutic target for CF not only to test the role of VCP in proteasome-

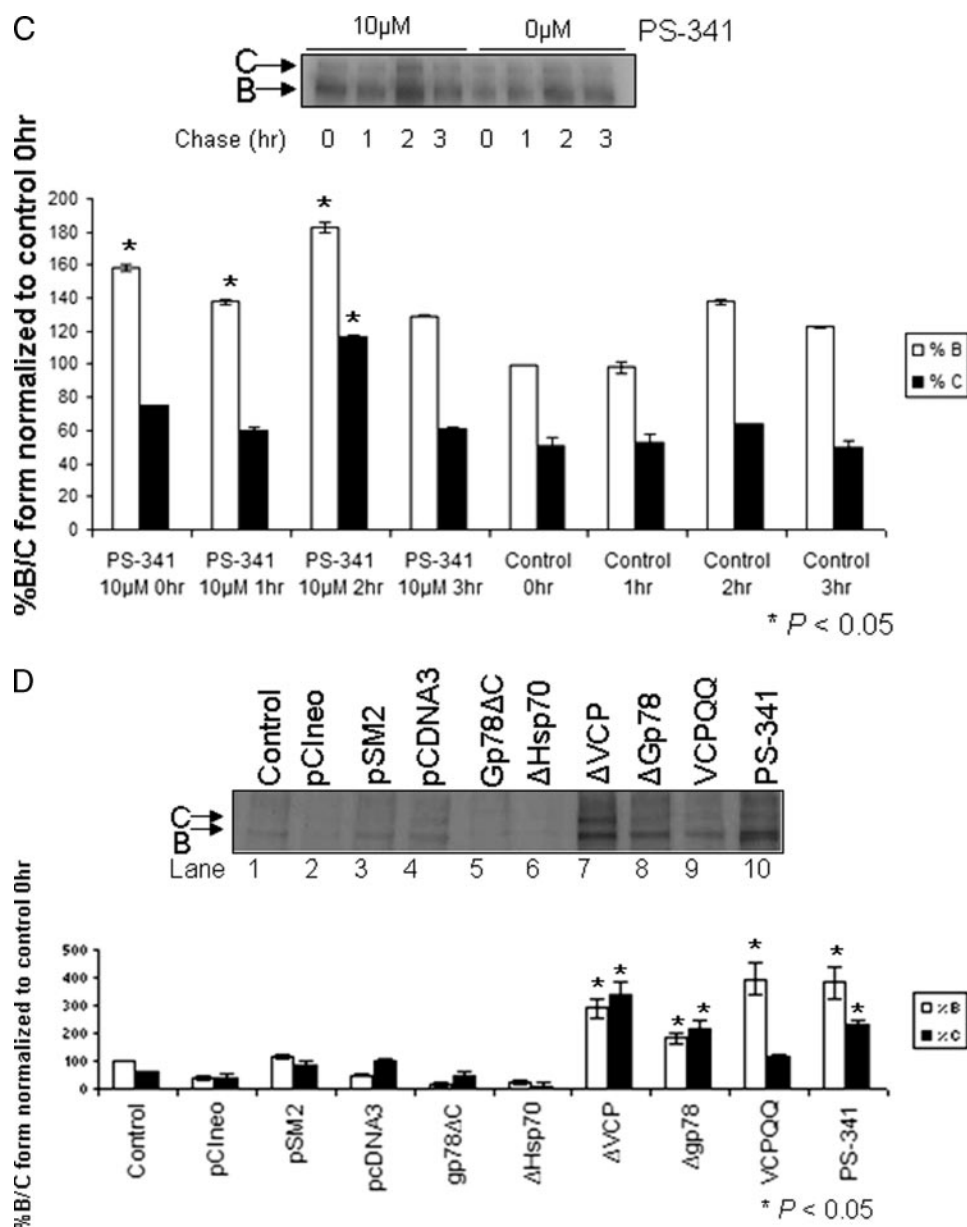


FIGURE 2—continued

mediated degradation of CFTR, but also because both VCP and proteasome inhibitors are known to stabilize $\text{I}\kappa\text{B}$, the inhibitor of the $\text{NF}\kappa\text{B}$ -mediated inflammatory response (16, 17). We used bortezomib (6-h treatment) at 10 μM , which leads to partial inhibition of protease activity in IB3-1 cells. Phase microscopic examination revealed no difference in morphology of treated and untreated monolayers (data not shown). To study the effect of bortezomib on another epithelial cell type homozygous for $\Delta F508$ -CFTR, we transfected CFTE cells (homozygous for $\Delta F508$ -CFTR) (18) with $\Delta F508$ -CFTR-GFP. After 42 h of transfection, cells were induced with bortezomib (10 μM) for 6 h. We observed a significant increase in the accumulation and stabilization of the B form with 10 μM bortezomib compared with the untreated control (Fig. 2C). S9 cells transfected with wt-CFTR and exposed to bortezomib similarly produced substantial amounts of mature band C (Fig. 2B).

To study the effect of inhibiting components of ubiquitination and proteasome degradation on ERAD, we first compared the relative basal levels of the immature B and mature C forms of $\Delta F508$ -CFTR in IB3-1

cells by metabolic labeling ($t = 2$ h) (Fig. 2D, lane 1). We observed no changes in the levels of the B and C forms of $\Delta F508$ -CFTR upon transfecting IB3-1 cells with empty vectors (pCIneo/pCIneo/pSM2) compared with the control (lanes 2–4). In contrast, both VCP and gp78 inhibition resulted in accumulation of the B form compared with the control, whereas the C form showed a more significant increase with VCP inhibition compared with a minimal increase with gp78 inhibition (lanes 7 and 8). Because VCP physically interacts with gp78 (8), it is expected that the gp78-VCP interaction may represent one way of coupling ubiquitination with retrotranslocation and degradation of $\Delta F508$ -CFTR. To evaluate the effect of this interaction on ERAD of $\Delta F508$ -CFTR, we used a gp78 Δ C construct deficient in the VCP-binding domain; no change in the levels of the B and C forms of $\Delta F508$ -CFTR compared with the control was observed (lane 5), suggesting that this gp78-VCP interaction is required for ERAD of $\Delta F508$ -CFTR. Moreover, the VCPQQ construct (deficient in AAA ATPase domains D1 and D2) partially rescued the B and C forms of $\Delta F508$ -CFTR (lane 9), indicating

Selective Inhibition of ERAD Rescues $\Delta F508$ -CFTR

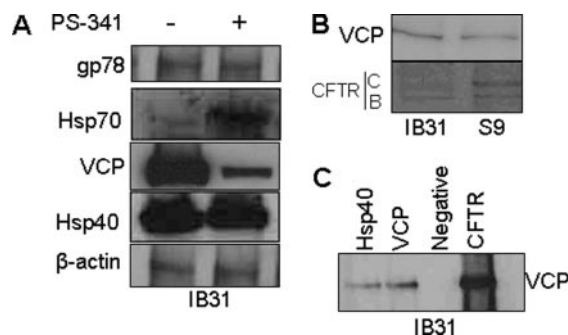


FIGURE 3. Proteasome inhibition by bortezomib/PS-341 modulates the VCP-CFTR immunocomplex. *A*, IB3-1 cells were treated with PS-341 for 6 h and immunoblotted for gp78, Hsp70, VCP, Hsp40, and β -actin as indicated. PS-341-mediated proteasome modulation induced Hsp70 and inhibited VCP with no change in gp78 and Hsp40. *B*, CFTR immunoprecipitates from IB3-1 and S9 cells (500 μ g/ml) were immunoblotted for VCP (upper panel) and CFTR (lower panel). *C*, CFTR, preimmune serum, VCP, and Hsp40 immunoprecipitates from IB3-1 cells were immunoblotted for VCP. VCP co-immunoprecipitated with wt-CFTR, $\Delta F508$ -CFTR, VCP, and Hsp40.

that two AAA ATPase domain are involved in ERAD of $\Delta F508$ -CFTR. The level of the C form was lower after transfection with the VCPQQ construct compared with complete VCP gene inhibition (Δ VCP) probably due to residual VCP AAA ATPase domain activity. Interference with Hsp70 expression (lane 6) did not rescue CFTR, which we expected because it is the increase in Hsp70 expression that promotes maturation of band B to C (19). The inhibition of proteasome-mediated degradation by bortezomib partially rescued $\Delta F508$ -CFTR from ERAD (lane 10). To investigate the effects of bortezomib on components of ERAD, IB3-1 cells were treated with bortezomib for 6 h and then immunoblotted for ERAD components. Induction of Hsp70 and inhibition of VCP were observed with no change in gp78 and Hsp40 (Fig. 3A).

p97/VCP Interacts with the CFTR Immunocomplex—To confirm that both $\Delta F508$ -CFTR and wt-CFTR are VCP substrates, we immunoprecipitated CFTR from IB3-1 and S9 total protein extracts (500 μ g/ml) using rabbit anti-CFTR polyclonal antibody 169 (15). VCP was co-immunoprecipitated with both $\Delta F508$ -CFTR and wt-CFTR (Fig. 3B, upper panel), indicating VCP to be the integral component of ERAD of CFTR. It is possible that VCP interacts with residual $\Delta F508$ -CFTR in the S9 cell line. Anti-VCP antibody was used as a positive control, and preimmune serum was used as a negative control for immunoprecipitation from IB3-1 cells. We also observed that VCP was co-immunoprecipitated with Hsp40 probably as part of the $\Delta F508$ -CFTR immunocomplex from IB3-1 cells (Fig. 3C).

To understand the mechanism of VCP-mediated ERAD of CFTR, we analyzed the interaction of VCP with other molecular chaperones known to be associated with $\Delta F508$ -CFTR or wt-CFTR degradation machinery. We immunoprecipitated CFTR, Hsp40, Hsp90, Hsc70, Hsp70, CHIP, and VCP from IB3-1 and S9 total protein extracts (500 μ g/ml) to evaluate relative VCP levels from each IB3-1 and S9 immunoprecipitate. We found that VCP was independently co-immunoprecipitated with $\Delta F508$ -CFTR, Hsp40, Hsp90, Hsc70, Hsp70, and CHIP from IB3-1 cells (Fig. 4A). Relatively higher amounts of VCP were pulled down with anti-Hsp40 and anti-Hsc70 antisera compared with other proteins, suggesting a stronger interaction or higher stoichiometry. VCP was pulled down together with Hsp90 and Hsp70 immunocomplexes from IB3-1 cells, but not from S9 cells (Fig. 4A). Moreover, VCP had a higher stoichiometry for these molecular chaperones in the presence of $\Delta F508$ -CFTR (IB3-1 cells) compared with wt-CFTR (S9 cells). Freshly isolated bronchial epithelial cells brushed from CF patients homozygous for $\Delta F508$ -CFTR were examined by immunoprecipitation of individual components of ERAD and immunoblotting for VCP or

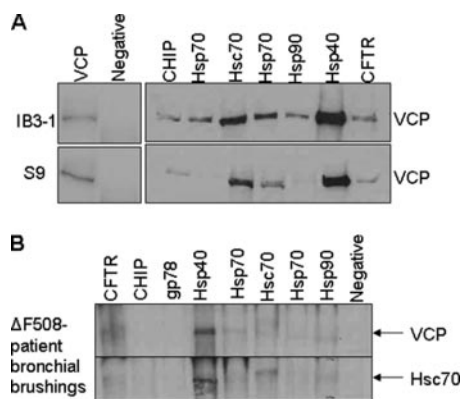


FIGURE 4. p97/VCP interacts with the CFTR immunocomplex. *A*, VCP, preimmune serum, CHIP, Hsp70, Hsc70, Hsp90, Hsp40, and CFTR were immunoprecipitated from IB3-1/S9 cells and then immunoblotted for VCP. VCP co-immunoprecipitated with both wt-CFTR and $\Delta F508$ -CFTR; moreover, VCP selectively co-immunoprecipitated with Hsp90, Hsp70, Hsp40, Hsc70, and CHIP in the presence of $\Delta F508$ -CFTR (IB3-1 cells) compared with wt-CFTR (S9 cells). *B*, CFTR, CHIP, gp78, Hsp40, Hsp70, Hsc70, and Hsp90 were immunoprecipitated from bronchial brushing of $\Delta F508$ CF subjects and immunoblotted for VCP or Hsc70. VCP and Hsc70 co-immunoprecipitated with $\Delta F508$ -CFTR, Hsp70, Hsc70, and Hsp40, but not with CHIP or gp78, from $\Delta F508$ CF subjects.

Hsc70 (Fig. 4B). Again, VCP and Hsc70 were prominent with anti-Hsp40 antibody.

VCP Inhibition and Bortezomib Treatment Induce Chloride Efflux—To confirm that $\Delta F508$ -CFTR rescue from ERAD leads to functional cell-surface chloride channels, we measured cAMP-stimulated halide efflux in IB3-1 cells. The IB3-1 cells were transfected with $\Delta F508$ -CFTR-GFP and cotransfected with Δ VCP, VCPQQ, Δ gp78, or gp78 Δ C or treated with bortezomib (1, 5, or 10 μ M) for 6 h. We observed minimal or no change in MQAE fluorescence (indicative of Cl^- channel activity) when stimulated by forskolin, although there was a significant change in fluorescence upon genistein treatment (Fig. 5A). Genistein is an isoflavonoid that directly activates CFTR chloride channels (20). We confirmed that the lack of forskolin-mediated CFTR channel activity in IB3-1 cells was due to the presence of endogenous cAMP by using CFTR inhibitor 172 (12) or the cAMP-specific inhibitor myristoylated protein kinase A inhibitor 14–22 amide (data not shown). We observed that acute exposure to genistein augmented chloride efflux with Δ VCP or Δ gp78 and upon treatment with 5 or 10 μ M bortezomib, suggesting a surface localization for $\Delta F508$ -CFTR (Fig. 5A). These results indicate that inhibiting VCP/gp78 or proteasome activity by bortezomib can rescue functional $\Delta F508$ -CFTR to the cell surface, resulting in a functional increase in cell-surface chloride transport detectable with agonist. Moreover, bortezomib/ Δ VCP and genistein had a synergistic effect on the rescue of functional $\Delta F508$ -CFTR from ERAD (Fig. 5A), probably by improving both CFTR trafficking and function. VCP inhibition rescued functional $\Delta F508$ -CFTR by $t = 8$ min (Fig. 5B). Together, these data demonstrate that we were able to express functional $\Delta F508$ -CFTR in IB3-1 cells by bortezomib treatment or selective inhibition of VCP.

VCP Inhibition and Bortezomib Treatment Down-regulate IL8 Levels and NF κ B Binding—It has been shown that human bronchial epithelial cells expressing $\Delta F508$ -CFTR generate more IL8 in response to tumor necrosis factor- α , IL1 β , or *Pseudomonas aeruginosa* (21, 22). After cell stimulation, I κ B α is phosphorylated and degraded by the 26 S proteasome, resulting in nuclear transport of NF κ B, followed by IL8 gene activation (23). To evaluate the effect of VCP-mediated ERAD on the NF κ B-mediated inflammatory response, we quantified IL8 levels in IB3-1 cells. The IB3-1 cells were transfected with the Δ VCP, VCPQQ, Δ gp78, or gp78 Δ C construct and treated with 5 μ M bortezomib or 5 mM 4-PBA, a histone deacetylase inhibitor that induces

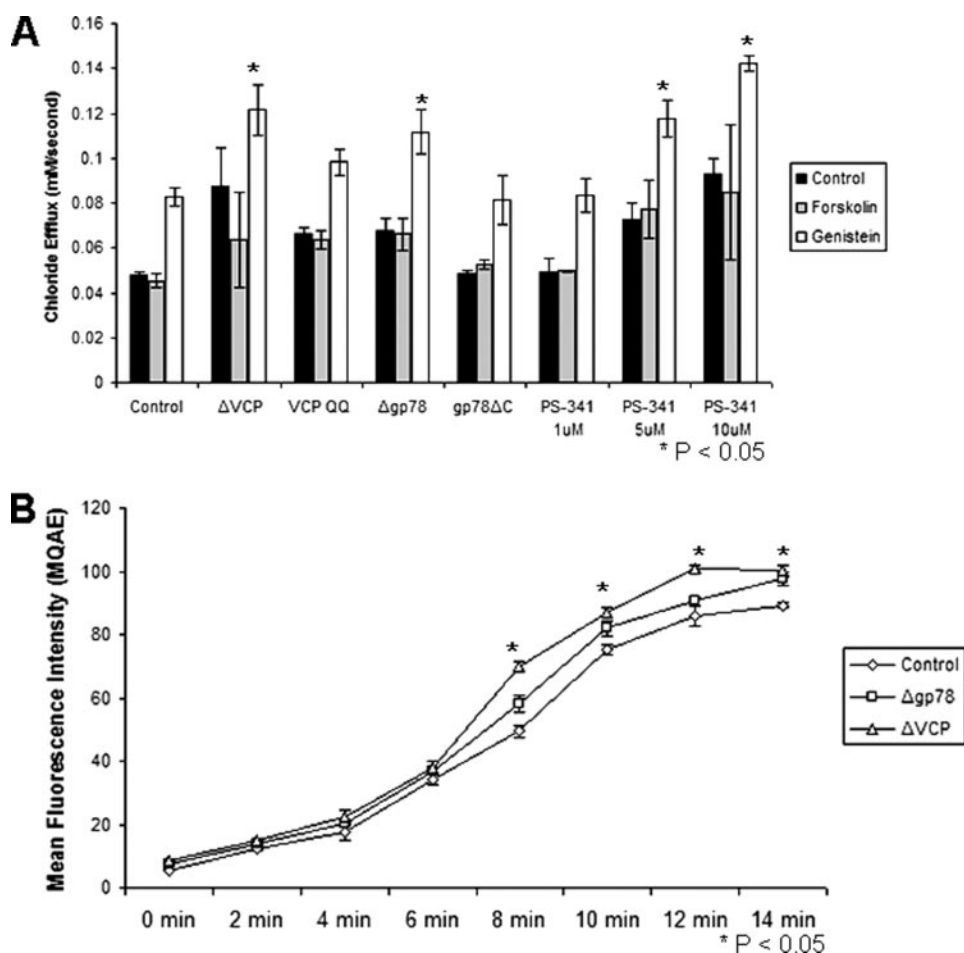


FIGURE 5. Induction of cAMP-mediated CFTR chloride efflux in IB3-1 cells by VCP/gp78 and bortezomib/PS-341. A, IB3-1 cells were transfected with $\Delta F508$ -CFTR and cotransfected with ΔVCP , VCPQQ, $\Delta gp78$, or gp78 ΔC or treated with PS-341 (0, 5, or 10 μM) for 6 h. Macroscopic halide permeability was monitored for transfected or PS-341-treated IB3-1 cells using a fluorescence-based (MQAE) assay. Each bar represents the mean change in chloride efflux (mm/s) \pm S.D. in a fixed microscopic area from three different experiments. ΔVCP , VCPQQ, $\Delta gp78$, and PS-341 (5 or 10 μM) significantly induced genistein-mediated chloride efflux. B, IB3-1 cells were transfected with $\Delta F508$ -CFTR and cotransfected with ΔVCP or $\Delta gp78$. Genistein was added at $t = 0$ min, and MQAE fluorescence was recorded every min from $t = 0$ to 14 min. Both VCP and gp78 inhibition led to a significant increase in MQAE fluorescence indicative of Cl^- activity. VCP inhibition rescued functional $\Delta F508$ -CFTR by $t = 8$ min. Data are the means \pm S.D. of three experiments.

Hsp70 (19). ΔVCP , $\Delta gp78$, and bortezomib significantly down-regulated IL8 levels compared with the control, VCPQQ, gp78 ΔC , and 4-PBA (Fig. 6A).

To confirm that down-regulation of IL8 levels is NF κ B-mediated, we evaluated NF κ B binding and IL8 levels in IB3-1 cells. IB3-1 cells were transfected (24 h) with ΔVCP , $\Delta F508$ -CFTR, or $\Delta CHOP$ or treated with 5 μM bortezomib (6 h), 5 μM MLN-273 (6 h; a novel small molecule proteasome inhibitor), or 5 mM 4-PBA (24 h). CHOP shRNA-mediated CHOP inhibition ($\Delta CHOP$) was used to suppress the oxidative stress in response to VCP or proteasome inhibition. Cells were induced with IL1 β (1 ng/ml) for 12 h. The supernatants and nuclear extracts from the same experiment were used to determine IL8 levels and NF κ B binding. NF κ B binding and IL8 levels were significantly inhibited by ΔVCP , MLN-273, and bortezomib compared with the control, $\Delta CHOP$, and 4-PBA. $\Delta CHOP$ and bortezomib had a synergistic effect on NF κ B binding and IL8 down-regulation (Fig. 6, B and C). Our results indicate that VCP or proteasome inhibition seems to be the most promising therapeutic strategy to restore CFTR trafficking and to inhibit I κ B α degradation simultaneously (16, 17) and hence NF κ B-mediated IL8 activation.

DISCUSSION

The ubiquitin-proteasome system consists of two steps. First, the target protein is conjugated with multi-ubiquitin molecules, which mark the substrate for destruction; second, the target protein is transferred to the 26 S proteasome, unfolded, and degraded. VCP is a multi-ubiquitin chain-targeting factor that is required for degradation of numerous ubiquitin-proteasome system substrates (24, 25). VCP is known to interact with the U-box domain-containing protein Ufd2 and

gp78 (ERAD-related ubiquitin-protein isopeptide ligase), resulting in ubiquitination of misfolded protein, followed by retranslocation to the proteasome (8, 26, 27). In our experiments, inhibition of VCP led to accumulation of CFTR in the ER, and a portion of the rescued mutant CFTR attained the C conformation, indicating passage through the Golgi. Parallel studies from other groups using yeast and mammalian systems demonstrated that Cdc48/VCP functions with the Ufd1-Nlp4 co-chaperone complex to bind ubiquitinated ERAD substrates and to deliver them to proteasomes (9, 28–30). The Cdc48/VCP chaperone complex binds ubiquitinated misfolded proteins and assists in their delivery from Hsp70 and Hsp90 to the proteasome (28, 29). The N-ethylmaleimide-sensitive factor and VCP are related AAA ATPase proteins implicated in membrane trafficking and organelle biogenesis. Although it was recently reported that VCP does not affect membrane trafficking (30), our observation of partial CFTR rescue by VCP inhibition indicates the following possibilities: 1) a small proportion of endogenous VCP can support the membrane trafficking function of specific proteins, but not ERAD; 2) the N-ethylmaleimide-sensitive factor or other related membrane trafficking components become active in response to accumulation of protein(s) in the ER; or 3) VCP inhibition may rescue trafficking proteins from proteasome-mediated degradation.

Two representative mammalian U-box proteins, Ufd2 and CHIP, interact with the molecular chaperones VCP and either Hsp90 or Hsc70, respectively, and are implicated in the degradation of damaged proteins (31). The combination of CHIP with Hsp90 mediates ubiquitylation of the glucocorticoid receptor, and CHIP together with Hsc70 is known to target immature CFTR for proteasome degradation (32, 33). We have shown here that VCP is directly associ-

Selective Inhibition of ERAD Rescues $\Delta F508$ -CFTR

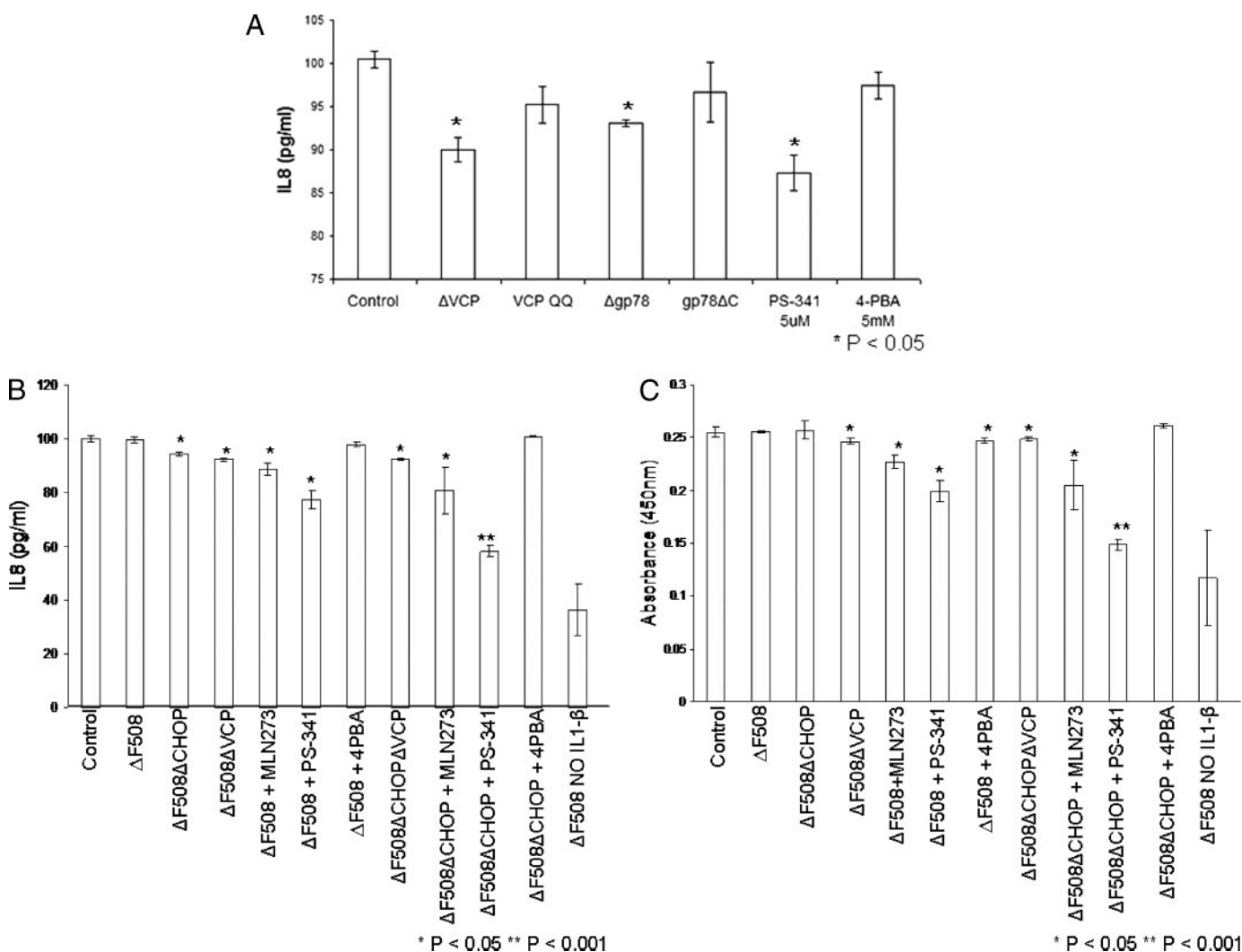


FIGURE 6. VCP inhibition and bortezomib/PS-341 treatment down-regulate IL8 levels. A, IB3-1 cells were transfected (48 h) with ΔVCP , VCPQQ, $\Delta gp78$, or gp78 ΔC or treated with 5 μM PS-341 (6 h) or 5 mM 4-PBA (48 h). Cells were induced with IL1 β (1 ng/ml) for 12 h. The percent average IL8 levels ($n = 3$) \pm S.D. of three independent experiments are shown. IL8 levels were significantly inhibited by ΔVCP , $\Delta gp78$, and PS-341 compared with the control, VCPQQ, gp78 ΔC , and 4-PBA. B, IB3-1 cells were transfected (24 h) with ΔVCP , $\Delta F508$ -CFTR, or $\Delta CHOP$ or treated with 5 μM PS-341 (6 h), 5 μM MLN-273 (6 h), or 5 mM 4-PBA (24 h). Cells were induced with IL1 β (1 ng/ml) for 12 h. The percent average IL8 levels ($n = 3$) \pm S.D. of three independent experiments are shown. IL8 levels were significantly inhibited by ΔVCP , MLN-273, and PS-341 compared with the control, $\Delta CHOP$, and 4-PBA. $\Delta CHOP$ and PS-341 had a synergistic effect on IL8 down-regulation. The no-IL1 β control ($\Delta F508 NO IL1-\beta$) represents basal IL8 levels. C, IB3-1 cells were transfected (24 h) with ΔVCP , $\Delta F508$ -CFTR, or $\Delta CHOP$ or treated with 5 μM PS-341 (6 h), 5 μM MLN-273 (6 h), or 5 mM 4-PBA (24 h). Cells were induced with IL1 β (1 ng/ml) for 12 h. The absorbance at 450 nm is directly proportional to bound NF κB . The binding of NF κB was significantly inhibited by ΔVCP , MLN-273, and PS-341 compared with the control, $\Delta CHOP$, and 4-PBA. $\Delta CHOP$ and PS-341 had a synergistic effect on NF κB binding. The no-IL1 β control ($\Delta F508 NO IL1-\beta$) represents basal NF κB binding. Each bar represents absorbance at 450 nm ($n = 3$) \pm S.D.

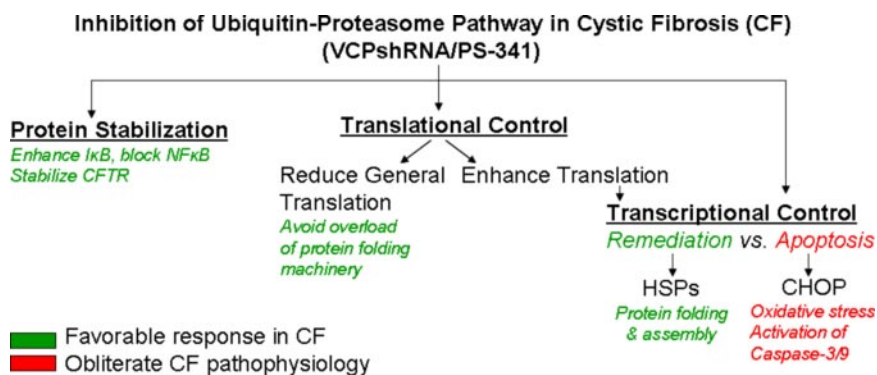
ated with CFTR and requisite for ERAD of CFTR, but it is not clear if both VCP- and CHIP-mediated pathways operate parallel to each other. Certainly VCP is also involved in retrotranslocation of tagged protein from the ER to the proteasome, indicating that it may be involved in steps after CHIP.

Inhibition of proteasome activity by *N*-acetyl-leucyl-leucyl-norleucinal (ALLN, 10 mg/ml) blocks $\Delta F508$ -CFTR degradation and drives accumulation of ubiquitinated forms of $\Delta F508$ -CFTR in Triton X-100-insoluble aggregates (34). It was reported recently that inhibition of the proteasome leads polyubiquitinated $\Delta F508$ -CFTR to aggregate because it can be extracted from the ER membrane by the VCP-Ufd1-Npl4 complex (7), but cannot be degraded by the proteasome (34). On the other hand, non-ubiquitinated $\Delta F508$ -CFTR that accumulates in response to inhibition of the Hsp70/CHIP ubiquitin-protein isopeptide ligase does not aggregate because it is inserted into the ER membrane and is bound by cytosolic Hsc70. Thus, whereas $\Delta F508$ -CFTR has a folding defect that prevents it from passing quality control and escaping the ER, it does not appear to be overly aggregation-prone, and cellular chaperones can

maintain it in a foldable state (35). The nature of the folding defect of $\Delta F508$ -CFTR and what causes it to be selected for proteasome degradation are not completely clear. To block the VCP-mediated proteasome degradation of CFTR, we used bortezomib. Proteasome inhibition with bortezomib or VCP inhibition partially rescued mature $\Delta F508$ -CFTR in IB3-1 cells. Bortezomib induced Hsp70 and down-regulated VCP protein expression. A recent report also demonstrated the inhibition of VCP by another proteasome inhibitor, hemin (36). Proteasome inhibition may also rescue trafficking protein(s) from degradation that may be involved in $\Delta F508$ -CFTR rescue to the cell surface.

The recent approval of bortezomib as a drug for refractory multiple myeloma (37–39) marks the beginning of a new era of regulation of protein catabolism for therapeutics. Bortezomib (pyrazolylcarbonyl-Phe-Leu-boronate) is an extremely potent, stable, reversible, and selective inhibitor of chymotryptic threonine protease activity (37). Bortezomib shows encouraging results when employed in hematological cancers and solid tumors. Bortezomib selectively induces NF κB -mediated apoptosis in cancer cells, whereas normal cells recover from proteasome

FIGURE 7. Inhibition of the ubiquitin-proteasome pathway in CF. Proteasome or VCP inhibition stabilizes I κ B and blocks NF κ B-mediated IL8 activation in addition to rescuing CFTR from degradation. Inhibition of the ubiquitin-proteasome pathway reduces general translation to avoid overload of the protein folding machinery, although it enhances translation and transcription of specific transcription factors such as heat shock proteins (HSPs) to enhance protein folding and assembly and CHOP to induce oxidative stress and apoptosis.



inhibition (40). Proteasome modulators have been shown recently to be of dual therapeutic importance in pharmacogenetic therapy of cystic fibrosis airways. The proteasome-modulating agents *N*-acetyl-leucyl-leucyl-norleucinal and doxorubicin enhance CFTR gene delivery and hence CFTR-mediated short circuit current. Moreover, these proteasome modulators also inhibit functional epithelial Na⁺ channel activity and currents independent of CFTR vector administration (41). We have shown here that bortezomib can rescue $\Delta F508$ -CFTR from ERAD and results in the appearance of mature CFTR. A main concern in considering the proteasome as a therapeutic target is the theoretical risk that multiple processes may be affected by proteasome inhibitors. ERAD is a central element of the secretory pathway and has major implications for the generation of various human diseases. ERAD was originally thought to exclusively degrade inefficiently folded and orphan secretory proteins. It is becoming clear that ERAD has important consequences for diverse aspects of cell physiology, including protein folding and transport, metabolic regulation, immune response, and ubiquitin-proteasome-dependent degradation (2). The risk of global suppression of proteasome degradation may be balanced by the favorable anti-inflammatory effect we observed.

Several studies have indicated that pulmonary inflammation may occur early in the course of CF, although the existence of primary inflammation is controversial (42, 43). It has been shown that human bronchial epithelial cells expressing $\Delta F508$ -CFTR generate more IL8 in response to tumor necrosis factor- α , IL1 β , or *P. aeruginosa* (21). These studies indicate that neutrophilic association with increased IL8 in the airways is a prominent early feature of CF and suggest that the exuberant airway inflammation is a component of the CF phenotype. In quiescent cells, NF κ B is sequestered to the cytoplasm by its interaction with a member of the I κ B inhibitory family that includes I κ B α and I κ B β . After cell stimulation, I κ B α is phosphorylated, polyubiquitinated, and degraded by 26 S proteasome activity. I κ B α degradation unmasks nuclear localization signals that allow NF κ B to be transported to the nucleus, resulting in activation of IL8 gene transcription (23). VCP inhibition and 5 μ M bortezomib significantly inhibited IL1 β -induced IL8 levels in IB3-1 cells from 100.49 \pm 0.95 pg/ml (control) to 89.96 \pm 1.43 (Δ VCP) and 87.27 \pm 2.05 pg/ml (bortezomib) ($p < 0.01$). VCP physically associates with I κ B α and the 26 S proteasome and targets I κ B α to the proteasome for degradation (16). The IL8 inhibition by VCP interference can be explained by I κ B α -mediated NF κ B inhibition. Bortezomib can enter mammalian cells and inhibit NF κ B activation and NF κ B-dependent gene expression. Bortezomib also inhibits tumor necrosis factor- α -induced gene expression of the cell-surface adhesion molecules E-selectin, ICAM-1 (intercellular adhesion molecule 1), and VCAM-1 (vascular cell adhesion molecule 1) on primary human umbilical vein endothelial cells (44, 45). In a rat model of streptococcal cell wall-induced polyarthritis (46), bortezomib attenuates the neutrophil-

predominant acute phase and markedly inhibits the progression of the T cell-dependent chronic phase of the inflammatory response (44).

Proteins unable to fold correctly cause ER stress and activate the UPR. The proteasome contributes to ERAD by relieving the ER stress. Accumulation of unfolded protein within the lumen of the ER leads to prolonged UPR activation, which in turn causes oxidative stress and finally cell death (47). To target the oxidative stress, we inhibited the major stress-inducible transcription factor CHOP/GADD153, which serves as a pro-apoptotic signal in response to the UPR (Fig. 7). The proteasome inhibitor is known to induce CHOP (48), although apoptosis was not apparent after proteasome or VCP inhibition in the present study. VCP itself was verified to be the major component of ER stress-induced apoptosis (47); hence, lack of apoptosis by VCP inhibition is apparent. Proteasome inhibition blocks NF κ B activation in response to exposure to cytokines or UV irradiation by stabilizing the labile I κ B α inhibitory protein (49). CHOP inhibition together with proteasome inhibition is synergistic in repression of NF κ B-mediated IL8 activation. Central to the pro-apoptotic function of proteasome inhibition is the transcriptional regulator CHOP, whereas VCP itself mediates ER stress-induced apoptosis.

VCP inhibition was more efficient in the rescue of the C form of CFTR compared with gp78 or proteasome inhibition. Mutant CFTR was relatively inert to stimulation by cAMP-mediated phosphorylation, but very sensitive to genistein, which directly activates both mutant and wild-type CFTRs. Because VCP is required for retrotranslocation of CFTR from the ER, VCP inhibition retains CFTR in the ER for trafficking to the plasma membrane. The gp78-mediated ubiquitination and proteasome degradation of CFTR occur after retrotranslocation from the ER; therefore, inhibition of these events is less effective in retaining CFTR in the ER. We conclude that VCP is the integral component of ERAD and ER stress pathways induced by the UPR in CF and may be central to the efficacy of CF drugs that target the ubiquitin-proteasome system. Modulating proteasome degradation by bortezomib or VCP shRNA rescues functional mutant CFTR to the cell surface and suppresses NF κ B-mediated IL8 activation. This ability to ameliorate secondary aspects of CF disease pathophysiology in addition to rescue of CFTR to the cell surface is promising for CF therapeutics. Moreover, the identification and selective modulation of ERAD components as potential therapeutics for a wide range of human diseases associated with ERAD promise an exciting and innovative area of investigation.

Acknowledgment—We thank Dr. William B. Guggino (Department of Physiology, The Johns Hopkins University) for critically reading the manuscript and Millennium Pharmaceuticals Inc., (Cambridge, MA) for providing proteasome inhibitor MLN-273.

REFERENCES

- Rock, K. L., and Goldberg, A. L. (1999) *Annu. Rev. Immunol.* **17**, 739–779
- Meusser, B., Hirsch, C., Jarosch, E., and Sommer, T. (2005) *Nat. Cell Biol.* **7**, 766–772
- Ward, C. L., Omura, S., and Kopito, R. R. (1995) *Cell* **83**, 121–127
- Rowe, S. M., Miller, S., and Sorscher, E. J. (2005) *N. Engl. J. Med.* **352**, 1992–2001
- Denning, G. M., Anderson, M. P., Amara, J. F., Marshall, J., Smith, A. E., and Welsh, M. J. (1992) *Nature* **358**, 761–764
- Gnann, A., Riordan, J. R., and Li, C. C. (2004) *J. Struct. Biol.* **146**, 44–57
- Ye, Y., Meyer, H. H., and Rapoport, T. A. (2003) *J. Cell Biol.* **162**, 71–84
- Zhong, X., Shen, Y., Ballar, P., Apostolou, A., Agami, R., and Fang, S. (2004) *J. Biol. Chem.* **279**, 45676–45684
- Gnann, A., Riordan, J. R., and Wolf, D. H. (2004) *Mol. Biol. Cell* **15**, 4125–4135
- Lim, M., McKenzie, K., Floyd, A. D., Kwon, E., and Zeitlin, P. L. (2004) *Am. J. Respir. Cell Mol. Biol.* **31**, 351–357
- Dignam, J. D., Lebovitz, R. M., and Roeder, R. G. (1983) *Nucleic Acids Res.* **11**, 1475–1489
- Ma, T., Thiagarajah, J. R., Yang, H., Sonawane, N. D., Folli, C., Galletta, L. J., and Verkman, A. S. (2002) *J. Clin. Investig.* **110**, 1651–1658
- Zeitlin, P. L., Lu, L., Rhim, J., Cutting, G., Stetten, G., Kieffer, K. A., Craig, R., and Guggino, W. B. (1991) *Am. J. Respir. Cell Mol. Biol.* **4**, 313–319
- Sharma, M., Benharouga, M., Hu, W., and Lukacs, G. L. (2001) *J. Biol. Chem.* **276**, 8942–8950
- Crawford, I., Maloney, P. C., Zeitlin, P. L., Guggino, W. B., Hyde, S. C., Turley, H., Gatter, K. C., Harris, A., and Higgins, C. F. (1991) *Proc. Natl. Acad. Sci. U. S. A.* **88**, 9262–9266
- Dai, R. M., Chen, E., Longo, D. L., Gorbea, C. M., and Li, C. C. (1998) *J. Biol. Chem.* **273**, 3562–3573
- Hideshima, T., Chauhan, D., Richardson, P., Mitsiades, C., Mitsiades, N., Hayashi, T., Munshi, N., Dang, L., Castro, A., Palombella, V., Adams, J., and Anderson, K. C. (2002) *J. Biol. Chem.* **277**, 16639–16647
- Kunzelmann, K., Schwiebert, E. M., Zeitlin, P. L., Kuo, W. L., Stanton, B. A., and Gruenert, D. C. (1993) *Am. J. Respir. Cell Mol. Biol.* **8**, 522–529
- Choo-Kang, L. R., and Zeitlin, P. L. (2001) *Am. J. Physiol.* **281**, L58–L68
- Moran, O., and Zegarra-Moran, O. (2005) *FEBS Lett.* **579**, 3979–3983
- DiMango, E., Zar, H. J., Bryan, R., and Prince, A. (1995) *J. Clin. Investig.* **96**, 2204–2210
- Srivastava, M., Eidelman, O., Zhang, J., Paweletz, C., Caohuy, H., Yang, Q., Jacobson, K. A., Heldman, E., Huang, W., Jozwik, C., Pollard, B. S., and Pollard, H. B. (2004) *Proc. Natl. Acad. Sci. U. S. A.* **101**, 7693–7698
- Siebenlist, U., Franzoso, G., and Brown, K. (1994) *Annu. Rev. Cell Biol.* **10**, 405–455
- Yen, C. H., Yang, Y. C., Ruscetti, S. K., Kirken, R. A., Dai, R. M., and Li, C. C. (2000) *J. Immunol.* **165**, 6372–6380
- Dai, R. M., and Li, C. C. (2001) *Nat. Cell Biol.* **3**, 740–744
- Kaneko, C., Hatakeyama, S., Matsumoto, M., Yada, M., Nakayama, K., and Nakayama, K. I. (2003) *Biochem. Biophys. Res. Commun.* **300**, 297–304
- Matsumoto, M., Yada, M., Hatakeyama, S., Ishimoto, H., Tanimura, T., Tsuji, S., Kakizuka, A., Kitagawa, M., and Nakayama, K. I. (2004) *EMBO J.* **23**, 659–669
- Ye, Y., Meyer, H. H., and Rapoport, T. A. (2001) *Nature* **414**, 652–656
- Bays, N. W., Wilhovskiy, S. K., Goradia, A., Hodgkiss-Harlow, K., and Hampton, R. Y. (2001) *Mol. Biol. Cell* **12**, 4114–4128
- Dalal, S., Rosser, M. F., Cyr, D. M., and Hanson, P. I. (2004) *Mol. Biol. Cell* **15**, 637–648
- Hatakeyama, S., Matsumoto, M., Yada, M., and Nakayama, K. I. (2004) *Genes Cells* **9**, 533–548
- Connell, P., Ballinger, C. A., Jiang, J., Wu, Y., Thompson, L. J., Hohfeld, J., and Patterson, C. (2001) *Nat. Cell Biol.* **3**, 93–96
- Meacham, G. C., Patterson, C., Zhang, W., Younger, J. M., and Cyr, D. M. (2001) *Nat. Cell Biol.* **3**, 100–105
- Johnston, J. A., Ward, C. L., and Kopito, R. R. (1998) *J. Cell Biol.* **143**, 1883–1898
- Younger, J. M., Ren, H. Y., Chen, L., Fan, C. Y., Fields, A., Patterson, C., and Cyr, D. M. (2004) *J. Cell Biol.* **167**, 1075–1085
- Oberdorf, J., Carlson, E. J., and Skach, W. R. (2006) *J. Cell Sci.* **119**, 303–313
- Mitchell, B. S. (2003) *N. Engl. J. Med.* **348**, 2597–2598
- Bross, P. F., Kane, R., Farrell, A. T., Abraham, S., Benson, K., Brower, M. E., Bradley, S., Gobburu, J. V., Goheer, A., Lee, S. L., Leighton, J., Liang, C. Y., Lostritto, R. T., McGuinn, W. D., Morse, D. E., Rahman, A., Rosario, L. A., Verbois, S. L., Williams, G., Wang, Y. C., and Pazdur, R. (2004) *Clin. Cancer Res.* **10**, 3954–3964
- Kane, R. C., Bross, P. F., Farrell, A. T., and Pazdur, R. (2003) *Oncologist* **8**, 508–513
- Adams, J. (2001) *Semin. Oncol.* **28**, 613–619
- Zhang, L. N., Karp, P., Gerard, C. J., Pastor, E., Laux, D., Munson, K., Yan, Z., Liu, X., Godwin, S., Thomas, C. P., Zabner, J., Shi, H., Caldwell, C. W., Peluso, R., Carter, B., and Engelhardt, J. F. (2004) *Mol. Ther.* **10**, 990–1002
- Khan, T. Z., Wagener, J. S., Bost, T., Martinez, J., Accurso, F. J., and Riches, D. W. (1995) *Am. J. Respir. Crit. Care Med.* **151**, 1075–1082
- Konstan, M. W., Hilliard, K. A., Norvell, T. M., and Berger, M. (1994) *Am. J. Respir. Crit. Care Med.* **150**, 448–454
- Palombella, V. J., Conner, E. M., Fuseler, J. W., Destree, A., Davis, J. M., Laroux, F. S., Wolf, R. E., Huang, J., Brand, S., Elliott, P. J., Lazarus, D., McCormack, T., Parent, L., Stein, R., Adams, J., and Grisham, M. B. (1998) *Proc. Natl. Acad. Sci. U. S. A.* **95**, 15671–15676
- Read, M. A., Neish, A. S., Luscinskas, F. W., Palombella, V. J., Maniatis, T., and Collins, T. (1995) *Immunity* **2**, 493–506
- Cromartie, W. J., Craddock, J. G., Schwab, J. H., Anderle, S. K., and Yang, C. H. (1977) *J. Exp. Med.* **146**, 1585–1602
- Rao, R. V., Poksay, K. S., Castro-Obregon, S., Schilling, B., Row, R. H., del Rio, G., Gibson, B. W., Ellerby, H. M., and Bredesen, D. E. (2004) *J. Biol. Chem.* **279**, 177–187
- Kitiphongspattana, K., Mathews, C. E., Leiter, E. H., and Gaskins, H. R. (2005) *J. Biol. Chem.* **280**, 15727–15734
- Jiang, H. Y., and Wek, R. C. (2005) *J. Biol. Chem.* **280**, 14189–14202